33RD INTERNATIONAL COSMIC RAY CONFERENCE, RIO DE JANEIRO 2013
THE ASTROPARTICLE PHYSICS CONFERENCE

ICRC 2013

# An anisotropy of galactic cosmic rays observed with GRAPES-3

A.OSHIMA[1], H.KOJIMA[3], S.SHIBATA[1], Y.HAYASHI[2], H.ANTIA[4], S.DUGAD[4], T.FUJII[7], S.K.GUPTA[4], S.KAWAKAMI[2], M.MINAMINO[2], P.K.MOHANTY[4], I.MORISHITA[9], T.NAKAMURA[6], T.NONAKA[7], S.OGIO[2], H.TAKAMARU[1], H.TANAKA[2], K.TANAKA[5], N.ITO[2], A.JAIN[4], T.MATSUYAMA[2], B.RAO[4], K.YAMAZAKI[2], N.YOSHIDA[1]

[1] *Chubu University*
[2] *Osaka City University*
[3] *Aichi Institute of Technology*
[4] *Tata Institute of Fundamental Research*
[5] *Hiroshima City University*
[6] *Kochi University*
[7] *Tokyo University*
[8] *Institute for Cosmic Ray Research University of Tokyo*
[9] *Asahi University*

*oshimaak@isc.chubu.ac.jp*

**Abstract:** Anisotropy in arrival direction of galactic cosmic rays were reported by several group Nagashima et al. and Hall et al., or more recently by ground based experiments such as Milagro and Tibet AS-gamma in sub-TeV energy region, and also IceCube in a few hundreds TeV region. A large scale anisotropy could be caused in several ways; the motion of the earth, large scale magnetic field structures, discrete distribution of cosmic ray sources, and so on. We have also reported a sidereal anisotropy of low energy cosmic rays in GeV energy observed with the large tracking muon detector of GRAPES-3 [1] [2]. Here we report a galactic cosmic ray anisotropy observed with GRAPES-3 air shower array in high energy region, specially in combination with the muon detectors for suppression of the contamination of primary hadrons.

**Keywords:** galactic, cosmic ray, anisotropy

## 1 Introduction

Observation of sidereal anisotropy of the high energy galactic cosmic ray is an effective method for determining the structure of magnetic field in the interstellar space near boundary of the heliosphere which is not understood yet very well. An anisotropy of galactic cosmic rays is thought to be reflect the general characteristic of propagation of galactic cosmic rays in the galactic magnetic fields. Nagashima et al. have studied sidereal time variation of cosmic rays for various energies. A number of experiment have studied the anisotropy, such as air shower experiment at Mt.Norikura (2750 m a.s.l), atmospheric muon measurements at Nagoya (sea level), at Sakashita (underground) and Hobart(underground, Australia). These measurements have indicated the existence of two kinds of sidereal time anisotropies, namely an intensity excess at sidereal time of 6 hour RA and deficit at 12 hour RA. These are called Tail-IN (TI) and Loss-cone (LC) anisotropies respectively. In addition, Hall et al. (1999) have analysed the data from many muon stations all over the world (sea level and underground) and have obtained results similar to that of Nagashima et al.

The observation of the sidereal variation of galactic cosmic rays at low rigidities is required for understand of the three dimensional direction of galactic anisotropy, which cannot be realised by observations only in the high rigidity region. From this point of view, it is worthwhile to investigate the existence of the sidereal variation of galactic cosmic rays.

The anisotropy of galactic cosmic ray intensity in the energy region of $\geq$ 10 TeV gives us an important information on the structure of galactic magnetic field of the heliosphere and the local interstellar space around the heliosphere, where cosmic rays propagate to the Earth. The anisotropy of galactic cosmic rays were measured via the sidereal daily variation of cosmic ray intensity by several ground based experiments. On the basis of the sidereal variation observed in the TeV region, most of the previous investigations reported that small amplitude and a phase of maximum somewhere between 23-3hours in the local sidereal time(LST). these observations are consistent with the large scale diffusive propagation of cosmic rays.

Here we present the new results of an anisotropy of the galactic cosmic gamma rays at very high energy region using the data of GRAPES-3 air shower array of 9-years from 2000 to 2008. We've used the muon data of GRAPES-3 large area tracking muon detector to discriminate the gamma induced air showers from nuclear induced ones effectively. For this purpose we applied a hadron rejection criteria on all the recorded air shower events in order to suppress a contamination of nuclear primary particles.

## 2 GRAPES-3 experiment

The experimental system of the GRAPES-3 (**G**amma **R**ay **A**stronomy at **P**eV **E**nergy**S** Phase-**3**) experiment consists of a densely packed array of scintillator detectors and a

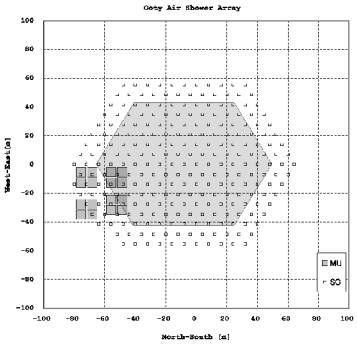


**Figure 1**: The GRAPES-3 experimental system with 257 scintillator detectors and 16 muon detector modules

large area tracking muon detector. The EAS array consists of 350 plastic scintillator detectors shown in Fig. 1, each of 1 $m^2$ in area. These detectors are deployed with an inter-detector separation of only 8 m. The array is being operated at Ooty in south India (11.4°N, 76.7°E, 2200 m altitude).

In order to achieve the lowest possible energy threshold, a simple 3-line coincidence of detectors has been used to generate the Level-0 trigger, which acts as the fast GATE and START for the analog to digital and time to digital converters (ADCs and TDCs), respectively. As expected, this trigger selects a large number of very small and local showers and also larger showers whose cores land very far from the physical area of the array. Therefore, it is also required that at least 10 out of the inner 127 detectors should have triggered their discriminators within 1 $\mu$s of the Level-0 trigger. This Level-1 trigger with an observed EAS rate of 13 Hz is used to record the charge (ADC) and the arrival time (TDC) of the pulses from each detector [4]. The pulse charge is later converted into the equivalent number of minimum-ionizing particles (MIPS) using the most probable charge for a single MIP measured using the trigger from a small area ($20\times20$ $cm^2$) scintillation counter telescope.

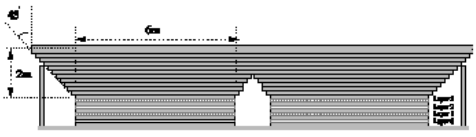

**Figure 2**: A muon station has four muon detector modules each consisting of 232 proportional counters. There are four muon stations inside the air shower array (Fig. 1).

The 560 $m^2$ GRAPES-3 muon detector [9] consists of 4 super-modules in Fig.2 , each in turn having 4 modules. Each module with a sensitive area of 35 $m^2$ consists of a total of 232 proportional counters (PRCs) arranged in 4 layers, with alternate layers placed in orthogonal directions. Two successive layers of PRCs are separated by 15 cm thick concrete. The energy threshold of 1 GeV for vertical muons, has been achieved by placing a total of 15 layers of concrete blocks (total absorber thickness $\sim$550 g.$cm^{-2}$) above the Layer-1. The concrete blocks have been arranged in the shape of an inverted pyramid to provide adequate shielding up to a zenith angle of 45°.

At higher energies, where observations have to be necessarily made with ground based particle detector arrays at high altitudes, the muon content of showers offers itself as a possible parameter to discriminate against air showers initiated by nuclear cosmic rays. As mentioned above, muon station of GRAPES-3 can measure the direction of muon content of a shower.

One of the most critical parameter in the study of direction of primary cosmic rays using a particle detector array is good angular resolution. This requires an accurate determination of the relative arrival time of the shower front at various detectors. The high density of the detectors in GRAPES-3 enabled an angular resolution of 0.7° to be obtained at energies as low as 30 TeV. Angular resolution of the GRAPES-3 was estimated by 2-D Gaussian fit to the Moon shadow data.

During the period of this analysis from 2000 to 2008, GRAPES-3 air shower array keeps stable good performance on the angular resolution. Fig. 3 shows the Moon shadow clearly seen in the all cosmic rays flux detected by GRAPES-3 air shower array at energies above 100TeV. The Moon shadow gives us a reasonable estimation of an angular resolution of GRAPES-3 air shower array of about $\sim$0.7° above 100 TeV.

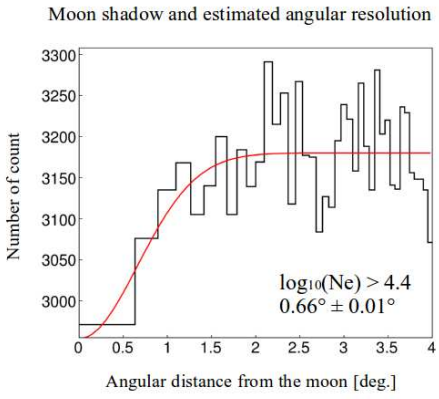


**Figure 3**: The deficit in cosmic ray intensity by an effect of the moon shadow in high energy region of above 100TeV. The data used for this analysis is from 2000 to 2008.

## 3 Hadron rejection and Analysis

The air showers that we observe on the earth are almost induced by charged cosmic rays and they have some amount of muon content with a certain lateral distribution depending on their energies. Therefore the air showers due to charged cosmic rays could provide huge noise for the gamma ray astronomy by the ground based experiments. However a charged cosmic rays could be identified precisely as a nuclear origin by measuring their muon content in the air shower using tracking muon detector. The GRAPES-3 tracking muon detector can record the hit pattern of muons and reconstruct the direction of the muons

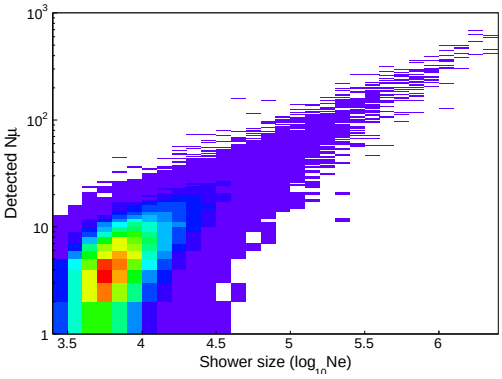


**Figure 4**: Distribution of detected muons of proton induced air showers in the CORSIKA simulation. The figure has been made with the following event selection; core location within the area of 20m from the center of muon station and zenith angle is witin 20 degrees.

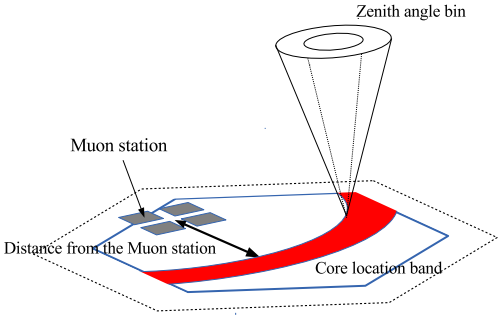


**Figure 5**: Classification of shower events for optimizing the performance of hadron rejection in this analysis.

with an angular resolution of about 6°. This implies that the tracking muon detector has a potential ability to distinguish primary gamma rays from large amount of charged primary nuclei. Then we tried to develop a strong and an effective hadron rejection criteria by taking advantage the tracking muon detector using CORSIKA monte carlo simulation.

This work was fully supported by COSIKA(COsmic Ray Simulations for KAskade) simulation code[8], which is widely used by high energy cosmic ray experiments around the world. The CORSIKA was set up with the parameter of QGSJII for high energy hadronic interaction and with GEISHA for low energy. The energy range of primary particles in the simulation was set from 5TeV to 1PeV with the spectral index of -2.7 for both proton and gamma primaries. All the simulated showers at the observation level of GRAPES-3 were reconstructed as real shower data, and the number of muons were counted by simulated GRAPES-3 tracking muon detectors. Since the high energy gamma rays can produce a certain amount of muons in air showers, just selecting muon zero showers as a gamma candidate can cause an elimination of gamma rays. Therefore we have to consider the distribution of the detected number of muons for both gamma primary and hadron primary and utilize the difference of shape of the distribution and optimize the detectable muon numbers in both gamma and proton induced showers. Fig.4 shows the detected muon distribution which were produced by the simulated proton induced air showers for different energies corresponding shower size.

Because the possible detected number of muons could be varying depending on their shower core location, primary energy and their zenith angles, we classified all the recorded air showers into bins with combinations of their core location, their estimated primary energies and their incident zenith angles as shown in the image of Fig.5, In the Fig.5, all the core location have been divided into 11 area bands of 10m width from the center of muon detector to the edge of the array. The zenith angle have also been classified into 5 bins of 10 degrees width from the zenith to 50 degrees. For each classified data set of air showers, we obtained the distribution of number of muons recorded by the muon detectors. We optimized the number of muons by considering both the hadron rejections and the gamma detections using CORSIKA simulation as mentioned above. Fig.6 shows a variation of both the detection efficiency for gamma ray induced showers and rejection efficiency for proton induced showers for different shower size and different distance from the muon detector. This condition will allow to detect above ∼90% gamma rays for all energy region above 100 TeV for primary gamma rays of a vertical incidence, while it can reject 99.999% protons. This means that the showers which survived our hadron rejection would be the candidates primary gamma rays.

## 4 Results

A total of $2.1\times10^9$ showers have been collected over a total live time of $27.8\times10^7$ s, spread over a 9-year period, from 2000 to 2008. After the hadron rejection, only the number of events of $1.8\times10^5$ was remained. For each EAS, the core location, the shower age 's' representing the steepness of the Nishimura-Kamata-Greisen (NKG) lateral distribution function and the shower size $N_e$ have been determined using the observed particle densities, following the minimization procedure discussed in detail by Tanaka et al [6]. Also, for each shower, the zenith ($\theta$) and the azimuth ($\phi$) angles have been calculated using the time information from the TDCs, also following the minimization procedure described by Tanaka et al [6].

The direction of each air shower events have been transformed into the equatorial coordinates, and have been binned from 0° to 360° in right ascension and from -90° to 90° in declination into square cells with a bin size of 3°. Each cell has been normalized by the averaged counts of its declination bands. The map data has been converted to the 2-D visualized map with smoothing process. The GRAPES-3 air shower array can observe the equatorial sky from -40° to 60° in declination. Fig.7 and Fig.8 show the sky map of significance values of the gamma ray candidates in the energy region of 100TeV and 290TeV.

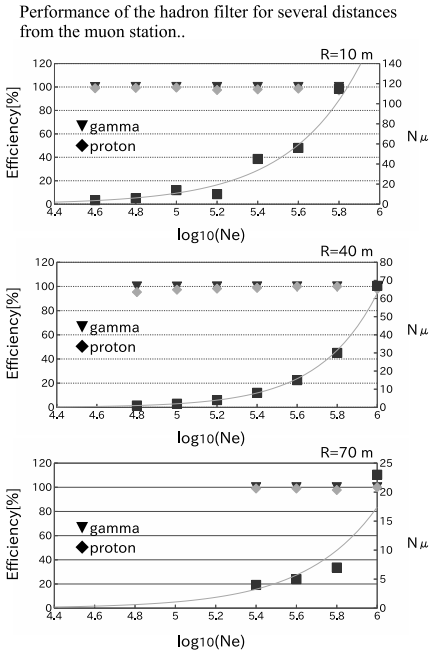


**Figure 6**: The conditions of hadron rejection have been applied with 99.999% rejection for above 100 TeV, performed for various shower size, area and zenith angles. Triangle shows the efficiency of primary gamma ray detection and diamond shows the proton rejection efficiency. Square shows the number of muons detected by the muon detector.

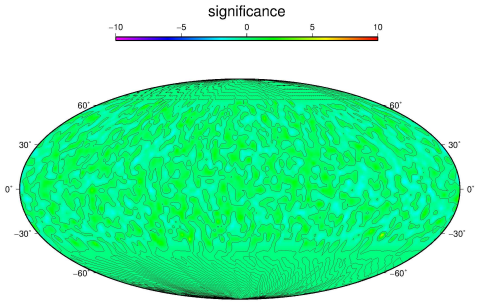


**Figure 7**: The sky map of gamma ray candidates of energy 100 TeV with an application of hadron rejection.

## 5 Summary

We developed a strong and an effective hadron rejection criteria by using CORSIKA monte carlo code. The hadron rejection criteria have been applied to all the recorded air shower events to suppress a contamination of hadron induced air showers. Because air showers due to primary nuclei contain large amount of muons with a certain lateral distribution, they play a large disturbance for the gamma ray astronomy performed by a ground based experiments. However very high energy gamma rays can produce air showers with some amount of muon contents too. Therefore simply selecting muon-zero air showers as gamma ray candidates which we reported previously [10] can possibly reject gamma ray induced air showers. Therefore we optimized hadron rejection criteria for each air showers and obtain a strong and effective hadron rejection efficiency and effective detection efficiency for gamma ray induced air showers. In this analysis using the data set of 9-years from 2000 to 2008, we calculated an anisotropy sky map of gamma ray candidates in the energy region of above 100 TeV and above 290 TeV with hadron rejection criteria. It has been founded that the uniform distribution of the arrival directions of the primary gamma ray candidates at high energy. The performance of the hadron rejection efficiency of the GRAPES-3 muon detector in this analysis can achieve 99.999% of hadronic primary cosmic rays.

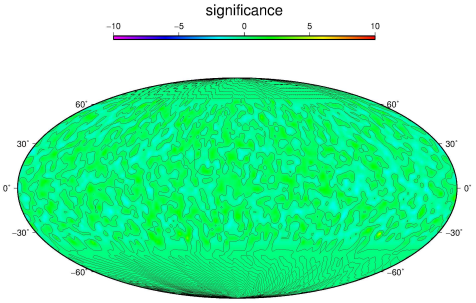


**Figure 8**: The sky map of gamma ray candidates of energy 290 TeV with an application of hadron rejection.

**Acknowledgment:** We thank all the GRAPES-3 collaborator in India for operation of the experiment. The air shower simulation and data analysis were carried out on the general-purpose PC farm and analysis servers at Center for Computational Astrophysics, National Astronomical Observatory of Japan.

## References

[1] Kojima H.,et al., Proc 28th ICRC, Tsukuba,Japan, 7, 3957 - 3960.,2003
[2] Kojima H.,et al., Proc 29th ICRC, Tsukuba,Japan, 2, 81 - 84.,2005
[3] S.K. Gupta, et al., J. Phys. G: Nucl. Part. Phys. 17 (1991) 1271.
[4] S.K. Gupta et al., Nucl. Instr. Methods A 540 (2005) 311.
[5] K. Greisen, Ann. Rev. Nuc. Sci. 10 (1960) 63.
[6] H. Tanaka et al., GRAPES-3 Preprint (2006).
[7] S.C. Tonwar, Workshop on Techniques in UHE $\gamma$-ray Astronomy, La Jolla, Eds: R.J. Protheroe & S.A. Stephens, Univ. of Adelaide (1985) 40.
[8] http://www-ik.fzk.de/corsika
[9] Y. Hayashi et al., Nucl. Instr. Methods A 545 (2005) 643.
[10] A. Oshima et al., Proc 32th ICRC, Beiging, China, 1, pp.109-112, 2011.